Acta Crystallographica Section D
Biological Crystallography
ISSN 1399-0047

Structural basis for the broad specificity of a new family of amino-acid racemases

Akbar Espaillat,[a,e]‡ César Carrasco-López,[b]‡ Noelia Bernardo-García,[b] Natalia Pietrosemoli,[c] Lisandro H. Otero,[b] Laura Álvarez,[a,e] Miguel A. de Pedro,[a] Florencio Pazos,[c] Brigid M. Davis,[d] Matthew K. Waldor,[d] Juan A. Hermoso[b]* and Felipe Cava[a,e]*

[a]Centro de Biología Molecular 'Severo Ochoa', Universidad Autónoma de Madrid–Consejo Superior de Investigaciones Científicas (CSIC), 28049 Madrid, Spain, [b]Department of Crystallography and Structural Biology, Instituto de Química-Física 'Rocasolano'–CSIC, 28006 Madrid, Spain, [c]Centro Nacional de Biotecnología–CSIC, 28049 Madrid, Spain, [d]Division of Infectious Diseases, Brigham and Women's Hospital and Department of Microbiology and Immunobiology, Harvard Medical School and HHMI, Boston, MA 02115, USA, and [e]Department of Molecular Biology and Laboratory for Molecular Infection Medicine Sweden, Umeå Centre for Microbial Research, Umeå University, Umeå, Sweden

‡ These authors contributed equally.

Correspondence e-mail: xjuan@iqfr.csic.es, felipe.cava@molbiol.umu.se

Received 2 August 2013
Accepted 5 September 2013

PDB References: BsrV, 4beu; ΔCl-BsrV, 4beq; Bsr_{Ah}, 4bf5; Alr_{Ah}, 4bhy

Broad-spectrum amino-acid racemases (Bsrs) enable bacteria to generate noncanonical D-amino acids, the roles of which in microbial physiology, including the modulation of cell-wall structure and the dissolution of biofilms, are just beginning to be appreciated. Here, extensive crystallographic, mutational, biochemical and bioinformatic studies were used to define the molecular features of the racemase BsrV that enable this enzyme to accommodate more diverse substrates than the related PLP-dependent alanine racemases. Conserved residues were identified that distinguish BsrV and a newly defined family of broad-spectrum racemases from alanine racemases, and these residues were found to be key mediators of the multispecificity of BrsV. Finally, the structural analysis of an additional Bsr that was identified in the bioinformatic analysis confirmed that the distinguishing features of BrsV are conserved among Bsr family members.

1. Introduction

In nature, the majority of D-amino acids (DAA) are found in bacterial cell walls, where D-Ala and D-Glu are key constituents of the short peptides that cross-link the glycan chains within the peptidoglycan (PG) polymer (Vollmer *et al.*, 2008). These DAA are produced from their corresponding L-enantiomers by highly specific alanine and glutamate amino-acid racemases (Alr and MurI), which have distinct structural and catalytic properties (Cava, Lam *et al.*, 2011). Alr (EC 5.1.1.1), which is the best characterized of these enzymes, is a cytoplasmic protein that requires the ubiquitous coenzyme pyroxidal-5-phosphate (PLP) as a cofactor (Richard *et al.*, 2009). Crystallographic studies of Alr from diverse organisms have enabled the identification of the structural determinants and spatial constrains that account for its mono-specificity (Couñago *et al.*, 2009; LeMagueres *et al.*, 2003, 2005; Noda *et al.*, 2004; Shaw *et al.*, 1997; Strych & Benedik, 2002; Wu *et al.*, 2008).

Recently, we demonstrated that diverse bacteria produce and release to the extracellular medium high amounts of DAA that are not canonical components of the cell wall (*e.g.* D-Ala and D-Glu; Cava, de Pedro *et al.*, 2011; Lam *et al.*, 2009). In *Vibrio cholerae*, the production of these noncanonical DAA (NCDAA) is dependent upon BsrV (VC1312), a periplasmic broad-spectrum racemase (Bsr) with high sequence homology (*E*-value of 1×10^{-25}, 28% identity) to the primary alanine racemase of *V. cholerae*, AlrV (VC0372; Fig. 1*a* and Supplementary Fig. S1*a*[1] Lam *et al.*, 2009). A subset of Alr-related racemases from other organisms have also been reported to accept multiple amino-acid substrates (Kino *et al.*, 2007; Lam

[1] Supporting information has been deposited in the IUCr electronic archive (Reference: DW5071).

et al., 2009; Matsui & Oikawa, 2010; Wu *et al.*, 2008). In *V. cholerae*, the presence of NCDAA negatively regulates cell-wall metabolism, at least in part owing to their incoporation into PG (Cava, de Pedro *et al.*, 2011; Cava, Lam *et al.*, 2011; Lam *et al.*, 2009). NCDAA have also been reported to influence biofilm stability (Kolodkin-Gal *et al.*, 2010), virulence (Anfora *et al.*, 2007) and sporulation (O'Connor & Zusman, 1997). Susceptibility to NCDAA seems to be more widespread than production of NCDAA, raising the possibility that some bacteria may produce and release NCDAA in order to influence nonproducing species within the same habitat (Cava, de Pedro *et al.*, 2011; Horcajo *et al.*, 2012). Given the important adaptative properties provided by NCDAA, a detailed investigation of multi-specific racemases will be critical to understand NCDAA-controlled processes and for the development of new drugs to combact pathogenic bacteria (Conti *et al.*, 2011).

Here, we explore the capacity of BsrV to utilize a wide variety of substrates using a combination of structural, biochemical, mutational and bioinformatic approaches. Finally, we also define and experimentally validate a molecular footprint of conserved residues that mediate the multi-specificity of BrsV and use this signature sequence to identify a large family of BsrV-like multi-specific racemases in bacteria.

2. Materials and methods

2.1. Microbiology

All *V. cholerae* strains used in this study were derived from the sequenced El Tor clinical isolate N16961 (Heidelberg *et al.*, 2000). Plasmids and primers, growth conditions and standard molecular-biology techniques are described in the Supporting Information.

2.2. Racemase activity assays

All racemase assays were performed in two fundamental steps: (i) the racemase reaction and (ii) the DAAO reaction coupled to peroxidase and 2,3-diaminophenazine or Marfey's (FDAA) derivatization (Fig. 1*b*). The formation of the colorimetric product was measured at 492 nm (see Supporting Information). The steady-state kinetics parameters were determined using *Microsoft Office* 2007 and *Solver Macro* (De Levie, 2001; see Supporting Information). For competition assays, FDAA derivatization of L and D forms of amino acids

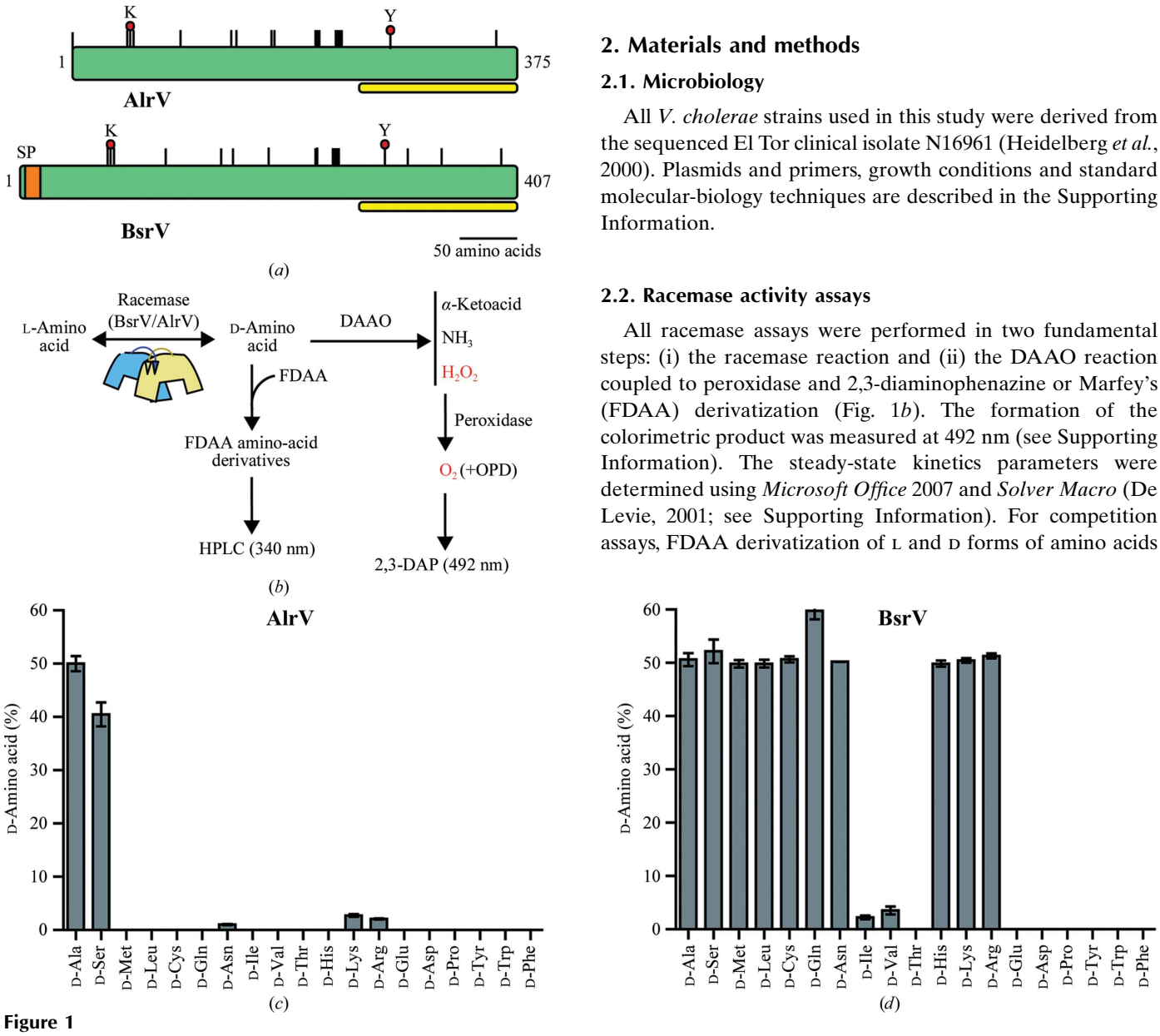

Figure 1
Biochemical comparison of AlrV and BsrV from *V. cholerae*. (*a*) Predicted protein features of the monospecific alanine racemase (AlrV) and broad-spectrum racemase (BsrV) from *V. cholerae* generated with the NCBI protein-analysis package. Dimerization motifs are in yellow. SP, signal peptide. Red circles pinpoint the catalytic Lys and Tyr residues. Vertical lines correspond to conserved functional residues (PLP binding, substrate binding, catalytic site and dimeric interface). (*b*) Schematic of the different methods used to assess amino-acid racemase activities (see §2). (*c*, *d*) D-Amino-acid accumulation in the presence of AlrV (*c*) and BsrV (*d*) after 90 min reactions with various substrates revealed through Marfey's derivatization. The results in (*c*) and (*d*) are the means ± SD of triplicates from two independent experiments. See also Supplementary Fig. S1.

Table 1
Kinetic parameters (K_m, k_{cat} and k_{cat}/K_m) of AlrV and BsrV for various amounts (1.25–60 m*M*) of L-amino-acid substrates were calculated using data obtained with 0.47 µ*M* purified racemase (see §2).

All kinetic constants must be considered as apparent values because of the impossibility of calculating initial enzyme velocities. The results are means ± SD of triplicates from two independent experiments. BsrV reaction kinetics for His and Cys were not determined (ND).

	K_m (m*M*)	k_{cat} (s^{-1})	k_{cat}/K_m (mM^{-1} s^{-1})
BrsV			
Ala	11 ± 2	1.68 ± 0.11	15.3×10^{-2}
Ser	28 ± 3	4.68 ± 0.21	16.7×10^{-2}
Met	11 ± 2	2.94 ± 0.04	26.7×10^{-2}
Leu	30 ± 7	2.30 ± 0.28	7.7×10^{-2}
Cys	ND	ND	ND
Gln	22 ± 3	2.59 ± 0.16	11.8×10^{-2}
Asn	15 ± 4	0.05 ± 0.004	0.3×10^{-2}
His	ND	ND	ND
Lys	9 ± 1	4.76 ± 0.11	52.9
Arg	18 ± 3	5.09 ± 0.11	28.3
AlrV			
Ala	1.5 ± 0.6	1.42 ± 0.003	94.5
Ser	17 ± 8	1.16 ± 0.0002	6.8

and HPLC analysis was performed (see Supporting Information).

2.3. Structural determination

Crystallization of BsrV, an $R_{173}N_{174}$/AA point mutant (ΔCl-BsrV), *Aeromonas hydrophila* Alr3 (a putative Bsr, renamed Bsr_{Ah}) and the putative primary alanine racemase from *A. hydrophila* (Alr_{Ah}) was performed using a high-throughput NanoDrop ExtY robot (Innovadyne Technologies Inc.) and the commercial Qiagen screens The JCSG+ Suite and The PACT Suite and the Hampton Research screens Index, Crystal Screen and Crystal Screen 2 following the sitting-drop vapour-diffusion method (see Supporting Information). X-ray data collection was performed at a synchrotron-radiation facility on beamlines ID29 and ID14-4 at the ESRF, Grenoble, France or on the X06SA beamline at SLS, Villigen, Switzerland (see Supporting Information). Data sets were collected using a PILATUS 6M or a Q315r ADSC X-ray detector, and were processed using *XDS* (Kabsch, 2010) and scaled using *SCALA* (Evans, 2006) from the *CCP*4 suite (Winn *et al.*, 2011). The structure was solved by the molecular-replacement method with *MOLREP* (Vagin & Teplyakov, 2010) from the *CCP*4 suite and was refined with *PHENIX* (Adams *et al.*, 2010) and manually improved using *Coot* (Emsley & Cowtan, 2004; see Supporting Information). The stereochemistry of the models was verified using *MolProbity* (Chen *et al.*, 2010).

2.4. Bioinformatic analyses

The identification of new putative broad-spectrum racemases and the residues responsible for substrate specificity was performed by searching with *BLAST* (Altschul *et al.*, 1997) against a nonredundant protein database and filtering, selecting only those mapped onto the UniProt database. The protein data set was aligned using *MUSCLE* (Edgar, 2004; v.3.8.31). The resulting multiple sequence alignment was filtered using the *Jalview* (Waterhouse *et al.*, 2009) tool (v.2.7). The identification of specificity-determining positions (SDPs) was carried out using the *JDet* package (see Supporting Information).

2.5. Accession numbers

The atomic coordinates and structure factors for BsrV, ΔCl-BsrV mutant, Bsr_{Ah} and Alr_{Ah} (PDB entries 4beu, 4beq, 4bf5 and 4bhy, respectively) have been deposited in the Protein Data Bank, Research Collaboratory for Structural Bioinformatics, Rutgers University, New Brunswick, New Jersey, USA (http://www.rcsb.org/).

3. Results

3.1. BsrV is a promiscuous paralogue of the *V. cholerae* alanine racemase AlrV

Comparisons of the substrate specificities of BsrV and AlrV, the presumed alanine-specific racemase from *V. cholerae*, revealed that BsrV is able to utilize a much broader range of substrates (Figs. 1*b*, 1*c* and 1*d*). Unlike AlrV, which only catalyzes the interconversion of L-Ala and L-Ser and their corresponding D forms (Fig. 1*c* and Supplementary Fig. S1*b*), BsrV reversibly racemizes ten of the 19 natural chiral amino acids known, including both non-β-branching aliphatic amino acids (Ala, Leu, Met, Ser, Cys, Gln and Asn) and positively charged amino acids (His, Lys and Arg) (Fig. 1*d* and Supplementary Figs. S1*c* and S1*d*). Additionally, it catalyzes the racemization of several amino acids that are not typically incorporated into proteins (Supplementary Fig. S1*e*). However, BsrV did not alter the chirality of negatively charged (*i.e.* Glu and Asp) or aromatic (*i.e.* Tyr, Trp and Phe) amino acids and displayed minimal activity towards β-branched aliphatic (*i.e.* Ile, Val and Thr) potential substrates (Fig. 1*d*).

3.2. Reaction kinetics of BsrV and AlrV

Kinetic analyses, using individual and pooled substrates, were also performed in order to better characterize the activities of BsrV and AlrV. Most analyses were performed using the His-tagged mature proteins used in structural studies because control assays performed with untagged mature BsrV showed that the affinity tag did not alter the activity of the enzyme (Supplementary Fig. S1*f*). The kinetic analyses revealed that the catalytic efficiency of BrsV (as reflected by k_{cat}/K_m) varies depending upon the amino-acid substrate and suggest that it acts more readily upon lysine, arginine and methionine than upon other substrates (Table 1). Assays using pooled substrates largely confirmed this idea: BsrV incubated with its ten potential L-amino-acid substrates efficiently formed D-Arg and D-Lys, but produced lower amounts of other DAA than when they were assayed singly (Supplementary Figs. S1*g* and S1*h*). Consequently, the high production of D-Met and D-Leu by *V. cholerae in vivo* (the principal products of BrsV; Lam *et al.*, 2009) is likely to reflect the relatively high availability of the corresponding L-amino acids.

Comparative analyses of BsrV and AlrV reaction kinetics revealed that the average k_{cat} of BsrV is higher than that of AlrV. However, the K_m values for BsrV were also around tenfold higher than the K_m of AlrV for alanine, its preferred substrate, and consequently k_{cat}/K_m for alanine racemization by AlrV is higher than that of BsrV for its substrate amino acids (Table 1). These facts fit well with the proposal that the development of catalytic multispecificity is often accompanied by a reduction in kinetic performance (Babtie *et al.*, 2010; Khersonsky *et al.*, 2006).

Table 2
Data-collection and refinement statistics.

Data set	BsrV	ΔCl-BsrV	Bsr_{Ah}	Alr_{Ah}
Space group	*C*2	*C*2	$P2_1$	$C222_1$
Unit-cell parameters				
a (Å)	96.62	95.99	56.67	110.80
b (Å)	51.09	50.99	81.85	134.74
c (Å)	76.73	76.46	78.28	192.15
α (°)	90	90	90	90
β (°)	101.15	100.69	98.97	90
γ (°)	90	90	90	90
X-ray source	ID29, ESRF	X06SA, SLS	ID14-4, ESRF	ID29, ESRF
Data processing				
Temperature (K)	100	100	100	100
Wavelength (Å)	0.95994	0.99987	0.93927	0.97901
Resolution (Å)	47.3–1.15 (1.21–1.15)	44.8–1.50 (1.58–1.50)	42.1–1.45 (1.53–1.45)	48.04–3.25 (3.43–3.25)
Measured reflections	483260	428625	1150270	75325
Unique reflections	128145	57665	124710	21300
Multiplicity	3.3 (3.1)	6.7 (6.6)	7.4 (7.0)	3.5 (3.6)
Completeness (%)	98.5 (98.5)	99.0 (99.0)	99.9 (99.7)	93.3 (95.4)
Average $I/\sigma(I)$	11.5 (4.3)	14.7 (4.2)	12.8 (2.5)	11.5 (1.8)
Molecules in asymmetric unit	1	1	2	4
Matthews coefficient ($Å^3$ Da^{-1})	2.2	2.2	1.6	2.3
Solvent content (%)	43.6	43.6	25.0	47.8
R_{merge}	0.05 (0.22)	0.08 (0.47)	0.09 (0.79)	0.09 (0.68)
Refinement				
Resolution range (Å)	47.3–1.15	47.1–1.50	42.1–1.45	47.32–3.25
Total No. of atoms	6670	6396	13365	10220
No. of protein non-H atoms	3074	2976	6238	9900
No. of ions (Cl^-)	1	—	2	—
No. of water molecules	532	447	931	177
R_{work}/R_{free}	0.16/0.17	0.15/0.17	0.19/0.21	0.26/0.29
R.m.s.d., bond length (Å)	0.010	0.010	0.004	0.009
R.m.s.d., bond angles (°)	1.368	1.297	0.620	1.110
Ramachandran statistics, residues in				
Most favoured regions (%)	97.10	97.17	97.09	84.85
Allowed regions (%)	2.99	2.83	2.91	10.20
Disallowed regions (%)	0.25	0.0	0.0	4.95
PDB code	4beu	4beq	4bf5	4bhy

3.3. The crystal structure reveals unique structural features in BsrV

Purified BsrV was crystallized and its structure was solved at atomic resolution (1.15 Å; Table 2). As observed for monospecific Alrs, BsrV folds as a globular homodimeric enzyme in which both monomers participate in the elaboration of the active sites (Fig. 2*a*). Analyses using the *DALI* server (Holm & Rosenström, 2010) indicate that the closest structural homologues of BsrV are alanine racemases from *Bacillus anthracis* (Alr_{Bax}; Couñago *et al.*, 2009; r.m.sd. of 2.0 Å for 361 C^α atoms) and *E. coli* (Alr_{Ec}; Wu *et al.*, 2008; r.m.s.d. of 2.5 Å for 347 C^α atoms). Since the crystallization of AlrV was unsuccessful, further comparative analyses of BsrV were performed with Alr_{Ec} (*E*-value of 3×10^{-157} to AlrV; Supplementary Fig. S1*a*). Superimposition of the BsrV and Alr_{Ec} structures readily reveals their extensive similarity; nonetheless, substantial differences are also apparent (Fig. 2*b* and Supplementary Figs. S2 and S3).

The entry channel to the catalytic site is approximately twofold wider in BsrV than in Alr_{Ec} (roughly 10 × 14 Å in BsrV compared with 7 × 9.5 Å in Alr_{Ec}; Fig. 2*b* and Supplementary Figs. S2*b* and S2*c*). This difference is a direct consequence of shorter loops in the side walls of the catalytic entry site in BsrV and of the different orientation of helix α10 (Fig. 2*b* and Supplementary Figs. S2*b* and S2*c*). In addition, the catalytic entry site has a negative charge in BsrV but not in Alr_{Ec} (Supplementary Fig. S2*d*), perhaps impeding the entry of acidic substrates into the catalytic site and thereby contributing to the selectivity of BsrV for neutral and basic amino acids. BsrV also contains a wider tunnel connecting the entry to the catalytic centre (the narrowest width of the BsrV tunnel is 9.0 Å compared with 6.3 Å in Alr_{Ec}).

The structure of BrsV also differs from that of Alr_{Ec} owing to the presence of an additional structural element formed from the sequence at the N-terminus of the protein (residues ^{24}APLHIDT^{30}). These amino acids fold into a stable, hinge-like complementary structure between monomers that shifts their relative positions (Figs. 2*b* and 2*c*). In BsrV monomers, the relative positions of the N-terminal domain (residues 24–279) and the C-terminal domain (residues 280–410) are offset by a 9° rotation compared with the equivalent domains in Alr_{Ec} (Fig. 2*c*), and an average displacement of 1.5 Å for the whole protein backbone is observed. Consequently, there are dramatic differences between the disposition and conformation of the active sites of BrsV and those of Alr_{Ec} (*e.g.* an increased distance between active sites from 37.6 Å in Alr to 45 Å in BsrV; Fig. 2*c*, right). The N-terminal structure of BrsV appears to be important for the activity of the enzyme, since a single mutation in this structure (P25E; Fig. 2*b* and Supplementary S3*a*) completely abolishes the activity of BrsV towards Ala and Met and dramatically impairs (70% reduction) its activity towards Arg.

3.4. The catalytic machinery of BsrV

In addition to the differences between the relative positions of protein domains in BsrV and Alr_{Ec}, comparative structural analyses revealed significant differences between the catalytic

centres of the two enzymes. Notably, the enzymes use different means to position their PLP cofactor (Fig. 3*a* and Supplementary Fig. S3*b*). In BsrV, a Tyr residue that is conserved among Alrs and is typically involved in coordination of the phosphate moiety of PLP is replaced by a proline residue (Pro391), thereby enlarging the space within the active site. Phosphate coordination in BsrV instead depends on Ser245 and Tyr208 and a network of interactions mediated by water molecules (Fig. 3*a* and Supplementary Fig. S3*b*). No differences are observed in the stabilization of the pyridoxal ring, where Arg260 stabilizes the N atom of the ring through its N^{ε} atom (2.82 Å).

The active site of BrsV also lacks an N-carboxylated lysine (Kcx) that in Alr_{Ec} and most alanine racemases stabilizes an arginine involved in substrate binding within the active site (Watanabe *et al.*, 2002). In BsrV, Kcx is replaced by Ala165 and the substrate-binding Arg (Arg173) is then stabilized in the active site by the presence of an ion (Fig. 3*a* and Supplementary Figs. S3*b* and S3*c*). Its tetracoordination (with one water molecule at 3.28 Å, the $N^{\delta 2}$ atom of Asn174 at 3.58 Å, the N^{ε} atom of Arg173 at 3.67 Å and the $N^{\eta 2}$ atom of Arg173 at 3.61 Å) and low *B* factor suggested that it was chloride (Cl^-; Fig. 3*a* and Supplementary S3*c*). A Cl^- ion has also been found in the monospecific alanine racemase Alr_{Bax}; however, unlike in BsrV, coordination of Cl^- in Alr_{Bax} is mediated by the same residues that interact with Kcx in Alr_{Ec} and other enzymes that contain Kcx (Couñago *et al.*, 2009). Furthermore, the position occupied by Asn174 in BsrV (Fig. 3*a*) contains hydrophobic residues (Leu and Ile) in Alr_{Ec}, Alr_{Bax} and other monospecific Alrs. Collectively, these analyses provide strong evidence that the presence of a negative charge near the catalytic residue is critical for amino-acid racemization by these enzymes; however, they also illuminate the differing catalytic environments in the active sites of enzymes with distinct specificities.

The relevance of the Cl^- to BsrV activity was further investigated by the structural and biochemical characterization of a BsrV $R_{173}N_{174}$/AA point mutant (ΔCl-BsrV). As expected, analysis of the crystal structure of ΔCl-BsrV (Table 2 and Fig. 3*b*) revealed that the Cl^- was absent. However, the structure of ΔCl-BsrV

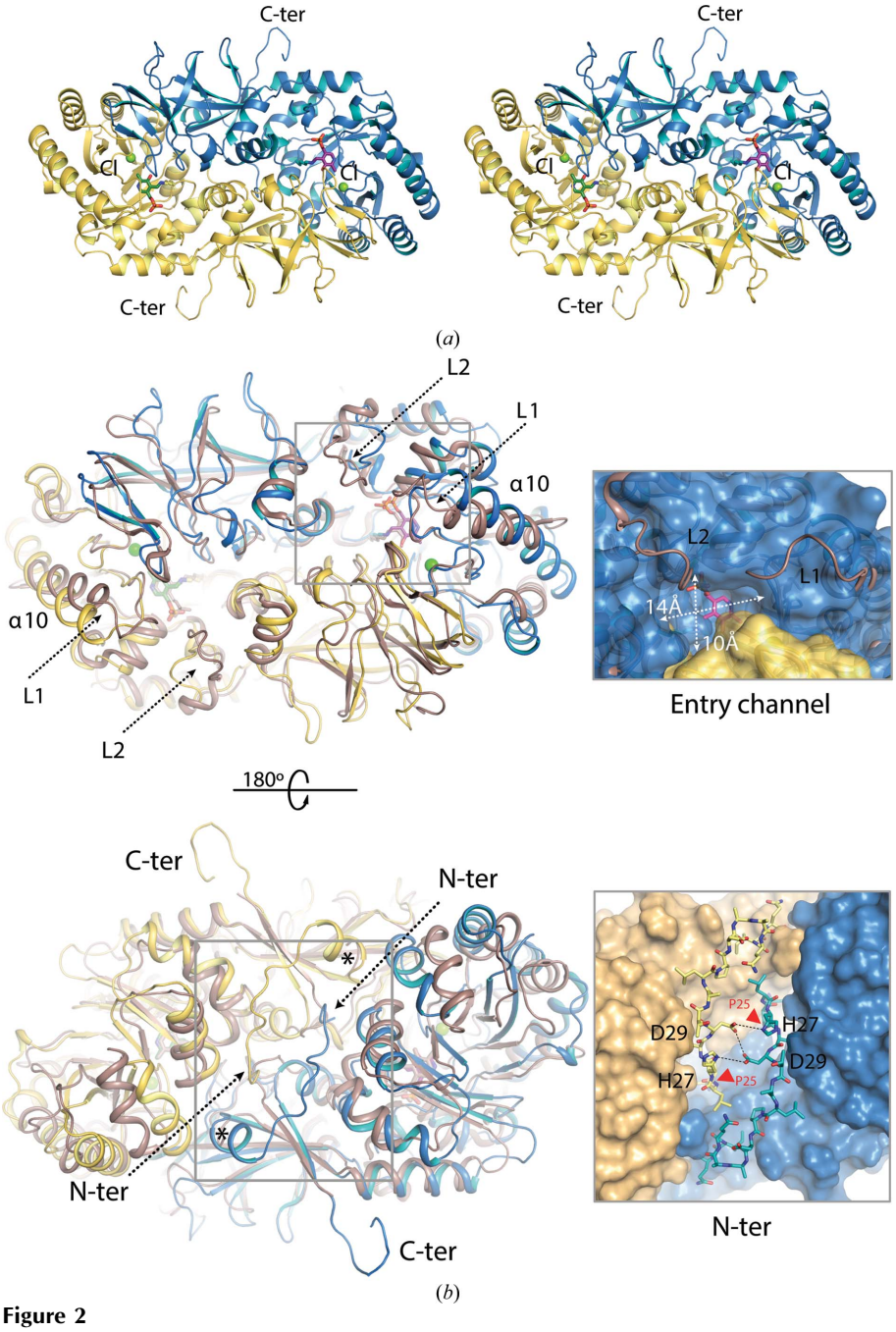

Figure 2
Three-dimensional structure of the BsrV dimer. (*a*) Crystal structure of a BsrV dimer with monomers depicted in yellow and blue. PLP molecules are shown in sticks and Cl^- ions are shown as green spheres. (*b*) Structural superimposition of BsrV coloured as in (*a*) and Ala racemase from *E. coli* (Alr_{Ec}) in brown. Loops L1 and L2 and α-helix α10 at the entry channel are labelled [six residues in L1 (204–210) and 11 residues in L2 (267–278) in BstV *versus* ten residues in L1 (159–169) and 18 residues (216–234) in L2 in Alr_{Ec}]. On the right, differences in their active-site cavities are shown. White arrows show the dimensions of the entrance of the BsrV cavity. At the bottom of (*b*), a 180° rotation view (back side) of the dimer is shown and the BsrV N-terminal insertion is highlighted in the box (bottom right). The position of the N-terminal residue for both monomers in the Alr_{Ec} structure is marked by an asterisk. In the close-up view of the back-side region of BsrV, the N-terminal insertion is shown as sticks. Polar interactions between the N-terminal extensions from both monomers are represented as dotted lines. The position of Pro25 is indicated by a red arrow.

was otherwise very similar to that of BsrV; the only minor changes observed were in the side chains of Tyr208 and His204 (Fig. 3*b*). As anticipated, ΔCl-BsrV had a highly reduced or no ability to racemize most amino acids (Fig. 3*c* and Supplementary Figs. S3*d* and S3*e*), consistent with Cl^- and Arg173 serving to replace Kcx in stabilizing a variety of substrates in the active site of BsrV.

3.5. Identification of molecular signatures that distinguish BsrV-like and Alr-like racemases

We hypothesized that the basis for the broad substrate tolerance of BsrV might be recognizable through sequence analysis and therefore searched for a molecular footprint of residues that are conserved among BsrV-like enzymes and differ from those found in monospecific alanine racemases. To initiate this analysis, a representative, nonredundant, set of PLP-dependent amino-acid racemase sequences (Alr and Bsr) from different bacteria were collected and aligned. Multiple sequence alignment (MSA; see §2) revealed differential conservation patterns that allowed clustering of proteins into three subfamilies (Fig. 4*a*). Subfamily 1 (in red) is composed of 84 proteins and includes AlrV, Alr_{Ec} and Alr2 (DadB) from *E. coli*, which have been experimentally confirmed as alanine-specific racemases (Fig. 1*c*; Faraci & Walsh, 1988; Lam *et al.*, 2009). Subfamily 2 (in blue) is comprised of 13 proteins, including BsrV (Alr2 from *V. cholerae*). Of the remaining 39 proteins in the data set, 24 proteins were grouped as subfamily 3 (in green). The 15 outlier proteins (in black) could not be assigned to any of the subfamilies (Fig. 4*a*). Based on the grouping of the characterized racemases, we assumed that the proteins in subfamily 1 are monospecific alanine racemases, while the proteins in subfamily 2 have a broader substrate spectrum. As no member of subfamily 3 or any of the 15 outlier proteins has been biochemically characterized, these proteins were not considered for further sequence analysis.

Further comparative analyses of subfamilies 1 and 2 (see Supporting Information) enabled the prediction of an initial set of 31 specificity-determining positions (SDPs) that appeared to typify the specific and broad-spectrum racemase subfamilies. After additional refinement with manual inspection of each potential SDP, this approach allowed the selection of 16 sites within these enzymes that appear to constitute a molecular footprint that can be used to distinguish alanine and broad-spectrum racemases (Fig. 4*b*; discussed further below). Mapping of the broad-spectrum-linked amino-acid loci to the BsrV structure revealed that these amino acids affect or reside within features that distinguish BsrV from AlrV, including placement of the entry sites (Arg119 and Arg121), the size of the catalytic entry site (Pro206, Tyr208, Lys216 and Tyr246) and the catalytic machinery (Cys70, Ala165, Asn167, Gly169, Asn174, Gly263, Asn348, Thr349 and Pro391; see Fig. 5*h*). Notably, specificity determinants were not found within the N-terminal extension of BsrV, although all of the putative broad-spectrum enzymes appear to possess this signature in the mature protein (relative to Alrs) as well as a putative signal sequence (Supplementary Table S3).

An expanded data set containing 2540 putative PLP racemases was similarly grouped into subfamilies and the identities of these families were determined based on the enrichment of proteins described as 'broad-spectrum' or 'specific' racemases in the previous analysis (see Supplementary Material). This strategy resulted in the identification of 74 BsrV-like racemases that had probably been mis-annotated previously as being specific racemases. Intriguingly, most Bsr candidates are found in Gram-negative marine bacteria, primarily (54.5%) in members of the Vibrionaceae family (Supplementary Table S4).

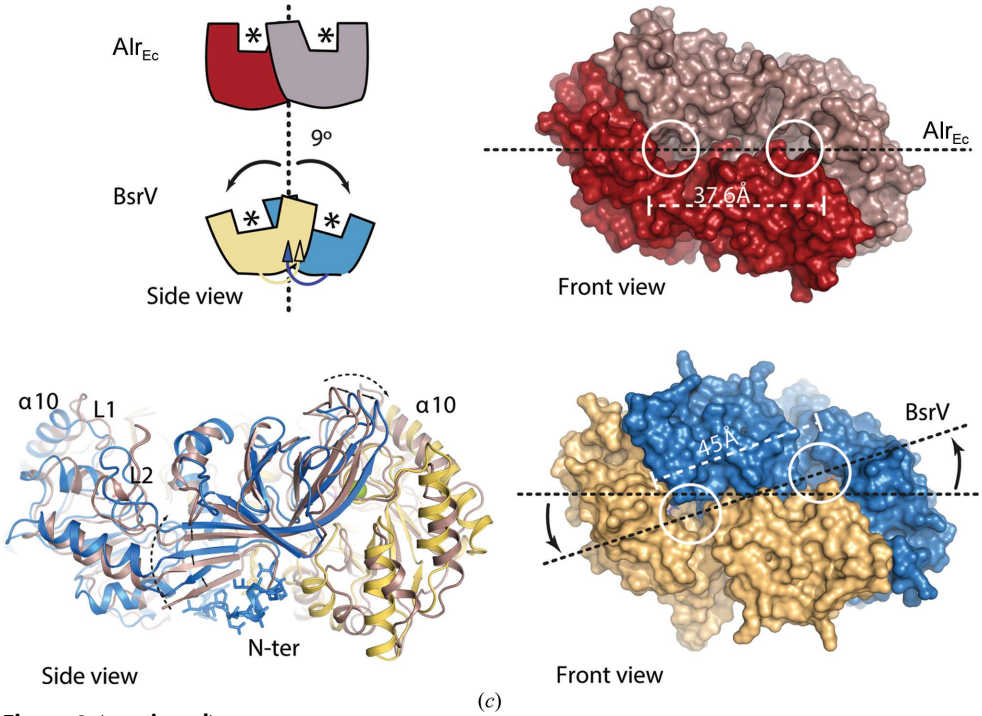

Figure 2 (continued)
(*c*) Different oligomeric arrangement between BsrV and Alr_{Ec} and its effect on the spatial distribution of the active sites. A schematic representation of the Alr_{Ec} and BsrV dimers is shown on the left; asterisks mark active sites. A rotation of 9° between monomers is produced by the N-terminal insertion in BsrV. Bottom left, structural superimposition of BsrV and Alr_{Ec} (brown cartoon). Displacement of the BsrV structural core by the N-terminal insertion (sticks) is represented by black arrows. Molecular surfaces for Alr_{Ec} and BsrV are shown on the right. The positions of active sites are marked by white circles and differences in distances and position of BsrV active sites *versus* Alr are highlighted. See also Supplementary Fig. S2.

3.6. The structure of the *A. hydrophila* broad-spectrum racemase mirrors that of BsrV

To validate our *in silico* identification of putative broad-spectrum racemases, we performed biochemical and structural characterization of *A. hydrophila* Alr3 (a putative Bsr, renamed Bsr_{Ah}) and the putative primary alanine racemase of *A. hydrophila* (Alr_{Ah}), which were identified from the 'broad-spectrum' and 'specific' subfamilies, respectively (Figs. 4*a* and 4*c*, Table 2 and Supplementary Fig. S4 and Table S4). As predicted, structural comparison revealed that Alr_{Ah} and Bsr_{Ah} differ in a manner analogous to that seen for BsrV and Alr_{Ec} (Supplementary Fig. S4), and Bsr_{Ah} exhibits all of the distinguishing structural features of BsrV [*i.e.* Cl^- instead of Kcx, a wider entry channel (shorter flanking loops) for the catalytic site, an N-terminal hinge-like extension and conserved signature residues; Fig. 4*c* and Supplementary Figs. S4*d*–S4*h*]. Bsr_{Ah} also resembles BsrV in its ability to discriminate between amino-acid substrates and displayed catalytic activity against an identical subset of natural amino acids (Supplementary Figs. S4*i* and S4*j*). Therefore, the distinct subfamilies of racemases evident in bioinformatic analyses appear to comprise a functionally distinct subset of amino-acid racemases with broad substrate specificity.

3.7. Molecular modelling of the docking of diverse amino-acid substrates within the BsrV and Alr_{Bs} active sites

To unveil the structural determinants that influence substrate stabilization in specific and broad-range racemases, we took advantage of the crystal structure of *B. stearothermophilus* alanine racemase (Alr_{Bs}) in complex with *N*-(5′-phosphopyridoxyl)-D-alanine (PLP-D-Ala; Watanabe *et al.*, 2002; PDB entry 1l6g) as the reference since this structure mimics the enzyme–substrate catalytic intermediate. We superimposed Alr_{Bs} in complex with PLP-D-Ala on BsrV and substituted the alanine analogue by all of the different kinds of amino-acid substrates, selecting the most stable conformation in each case (Figs. 5*a*–5*f*). Whilst Alr_{Bs} could only accommodate alanine and serine (not shown) in its catalytic site (Figs. 5*b*, 5*d* and 5*f* and Supplementary Table S5*b*), the BsrV catalytic pocket appears to accommodate all ten amino acids found to be racemized by this enzyme (Figs. 5*a*, 5*c* and 5*e*). Furthermore, in full agreement with the substrate specificity of BsrV, the remaining nine amino acids present multiple steric clashes when forced to fit into the active site of the enzyme (Supplementary Fig. S5*a*).

The docking analysis supported two overlapping mechanisms for amino-acid stabilization by BsrV: one for aliphatic

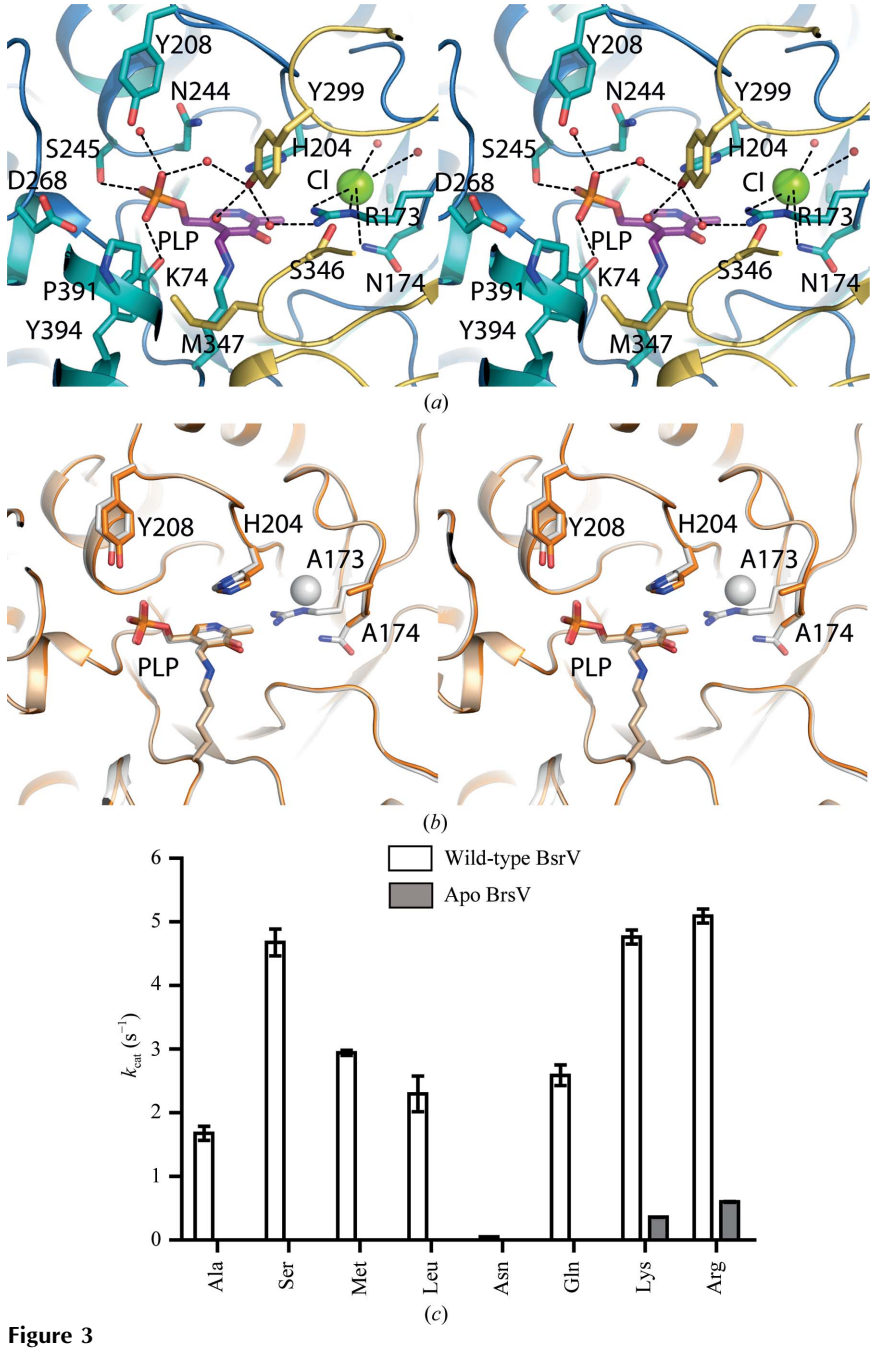

Figure 3
BsrV and ΔCl-BsrV active-site structures and kinetic parameters. (*a*) Stereoview of the BsrV active site. Relevant residues and PLP are shown as sticks; water molecules and Cl^- ions are shown as red and green spheres, respectively. (*b*) Stereoview showing the structural superimposition of the active sites of wild-type BsrV (shown as a white transparency) and ΔCl-BsrV ($R_{173}N_{174}$/AA) (coloured orange). No other significant changes apart from the double mutation and consequent Cl^- loss (white sphere) are apparent. (*c*) Comparison between the k_{cat} of ΔCl-BsrV and BsrV for different racemizable amino acids. The results in (*c*) are means ± SD of triplicates from two independent experiments. See also Supplementary Fig. S3.

residues and another for basic amino acids. Aliphatic amino acids (Ala, Ser, Cys, Leu, Gln and Met) are likely to be stabilized in the active site of BrsV through polar interactions between their carboxylate moiety and Arg173, Tyr299′ and Tyr318′, in a similar way to that defined for Ala in Alr_{Bs} (Figs. 5*a* and 5*b*). In addition, the amino-acid side chains are stabilized through hydrophobic interactions with Met347′ in BsrV (Figs. 5*a*, 5*c* and 5*e*). Basic amino acids (Arg, Lys and Orn) are stabilized by the same interactions at their carboxylate moieties and, in addition, by hydrogen bonding to Tyr394 and by electrostatic interactions with Asp268 and the PLP phosphate group (Fig. 5*e*).

Furthermore, docking results neatly explain why BsrV, but not Alrs, racemizes long aliphatic and basic residues. In Alrs, a Tyr residue (Tyr354 in Alr_{Bs}) closes the active-site cavity, which accommodates the short chain of the Ala residue (Fig. 5*b*) but produces steric clashes when longer aliphatic, or basic, residues are docked (Figs. 5*d* and 5*f*). The presence of a Pro residue (Pro391) at the equivalent position in BsrV makes sufficient additional space for the proper fitting of both long aliphatic and basic residues (Fig. 5*c* and 5*e*).

The differential efficiency of BsrV for its substrates was also in agreement with the docking results. Indeed, the lower activity values found for His and Asn (Supplementary Fig.

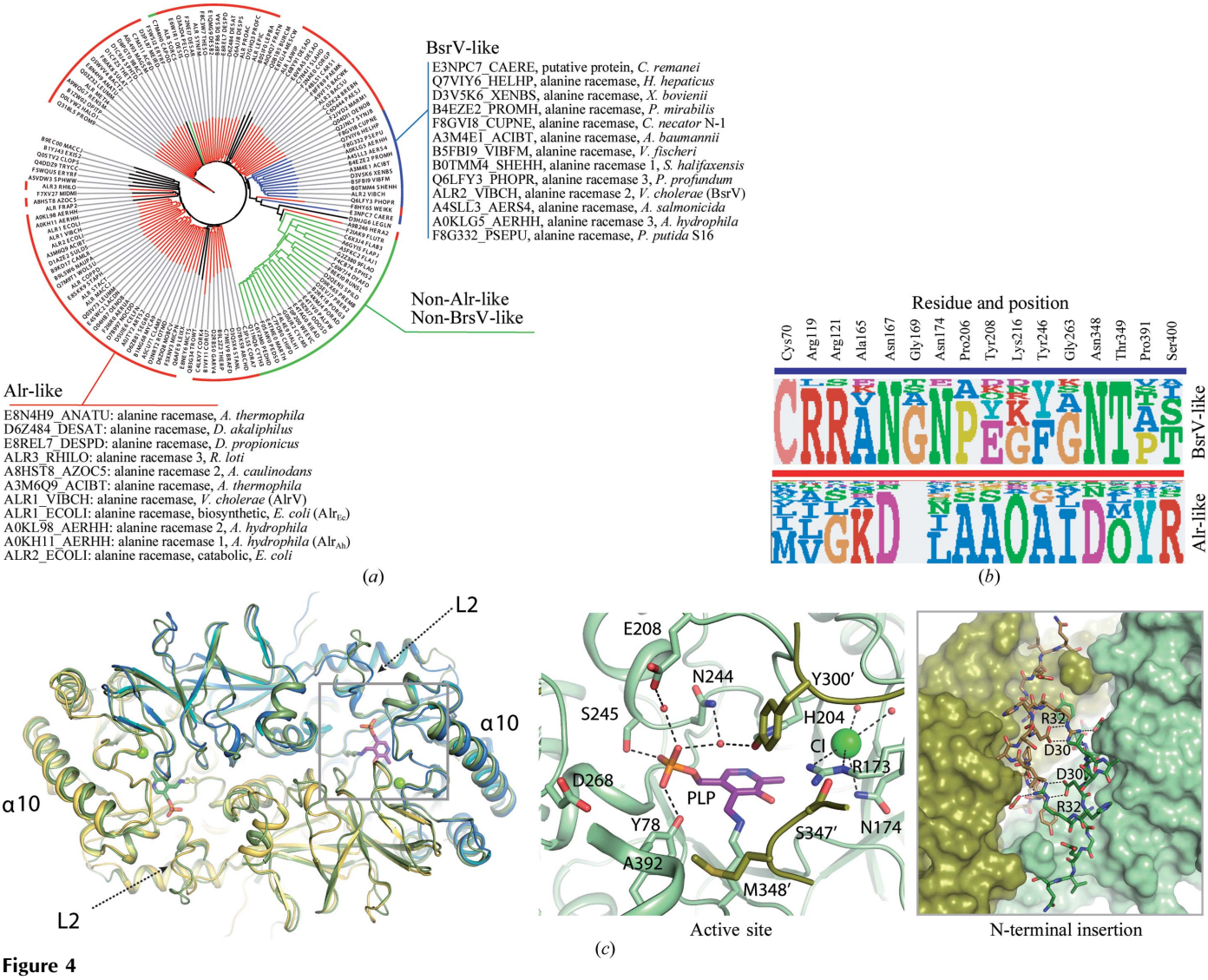

Figure 4

The identification of 16 residues that constitute the molecular footprint for BsrV multispecificity and experimental validation. (*a*) Tree of BsrV orthologues obtained through bioinformatic sequence analysis (see §2). Alr-like enzymes are highlighted in red, Bsr-like enzymes in blue and non-Alr-like, non-Bsr-like enzymes in green; 15 outlier proteins that do not group with any of these families are shown in black. All Bsr-like family members (including BsrV) and a small subset of Alr-like enzymes (including AlrV and Alr_{Ec}) are listed. (*b*) Molecular footprint. Sequence composition (displayed as sequence logos) of the specificity-determining positions for Alr/BsrV-like racemases. The specific residues and their positions are listed at the top. (*c*) Structural analysis of the broad-spectrum racemase from *A. hydrophila* (Bsr_{Ah}). A structural superimposition of BsrV with Bsr_{Ah} is shown on the left. Loop L2 and the α-helix α10 at the entry channel are labelled. The central panel shows a close-up view of the Bsr_{Ah} catalytic site. Relevant residues and PLP are shown as sticks; water molecules and Cl^- ions are shown as red and green spheres, respectively. In the right box, a close-up view of the back-side region (180° rotation view) of Bsr_{Ah} with the N-terminal insertion in stick representation is shown. Polar interactions between relevant residues of the N-terminal extensions from both monomers are represented as dotted lines. See also Supplementary Fig. S4.

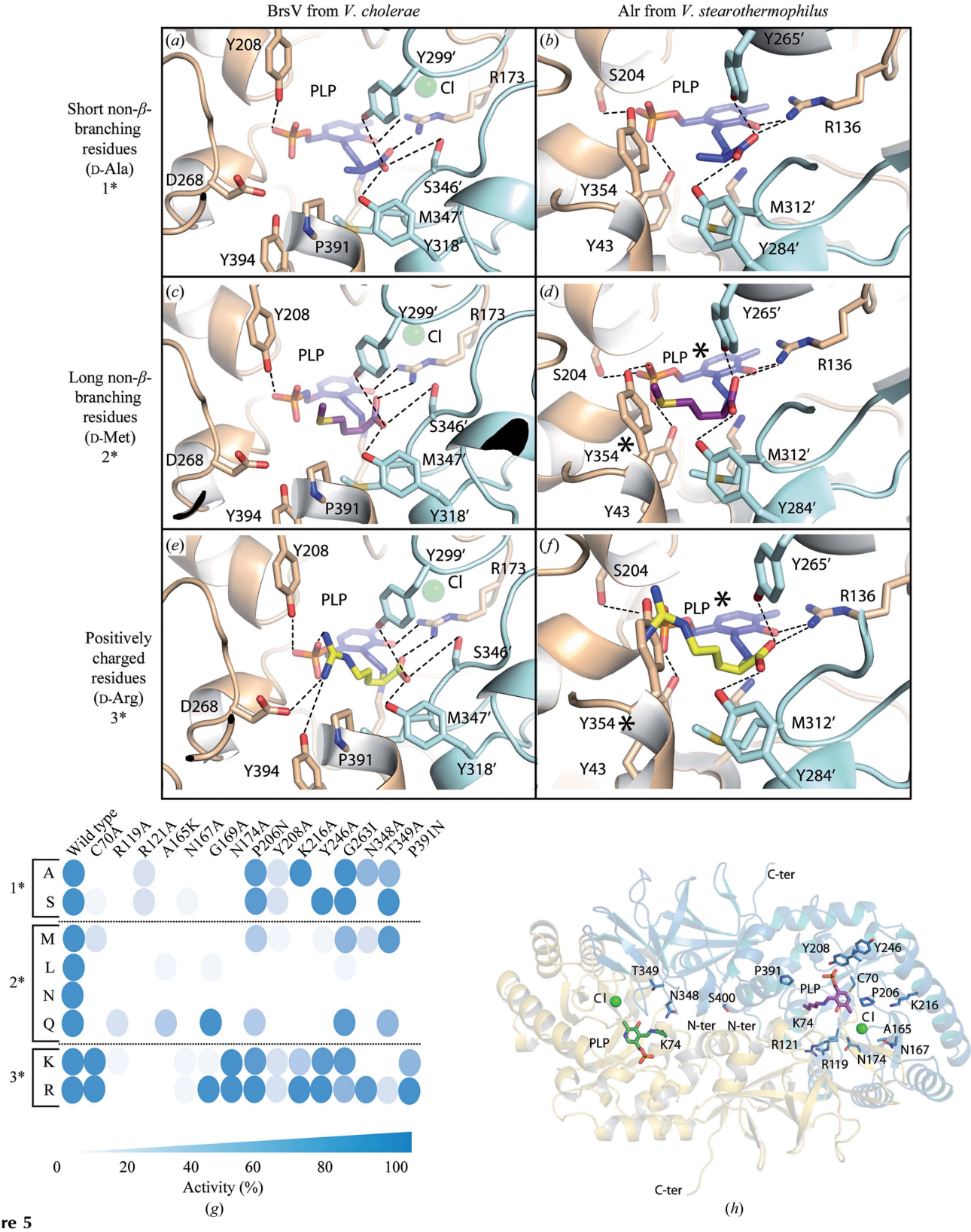

Figure 5
DAA recognition by BsrV from *V. cholerae versus* Alr from *B. stearothermophilus*. Docked models of enzyme–substrate catalytic intermediates (BsrV and Alr_{Bs}) for (*a*, *b*) short non-β-branching residues (D-Ala, shown in stick representation with C atoms coloured blue) (1*), (*c*, *d*) long non-β-branching residues (D-Met, shown in stick representation with C atoms coloured magenta) (2*) and (*e*, *f*) positively charged residues (D-Arg, shown in stick representation with C atoms coloured yellow) (3*). Protein residues involved in substrate recognition are labelled and interactions are highlighted as dotted lines. Substrates clashes are labelled by an asterisk. (*g*) Schematic of specific activity (relative to wild-type BsrV; left column) of BsrV single mutants in the 'signature' SDP. The results correspond to means of triplicates. (*h*) Location of the SDP within the BrsV structure. See also Supplementary Fig. S5.

Table 3
Structural analysis of the molecular footprint of BrsV.

Mutation	Protein region	Structural explanation
C70A	Active site	Structural stabilization of active site by a disulfide bridge
R119A	N-terminal insertion	Arg119 is involved in salt-bridge interactions allowing N-terminal insertion in BsrV
R121A	N-terminal insertion	Arg121 is involved in salt-bridge interactions allowing N-terminal insertion in BsrV
A165K	Active site	Ala at this position allows the correct stabilization of the Cl^- ion by Arg173 and Asn174 (in Alrs, this position is occupied by the *N*-carboxylated Lys)
N167A	Active site	Structural stabilization of loop involved in Cl^- coordination
G169A	Active site	Loop involved in Cl^- coordination
N174A	Active site	Residue involved in Cl^- coordination
P206N	Entry loops	Structural stabilization of the L1 loop (involved in substrate entry)
Y208A	Entry loops	Stabilization of the PLP phosphate group
K216A	Entry loops	Salt-bridge interaction stabilizing α10 at the entry
Y246A	Entry loops	Mutation will block movement of the r2 region
G263I	Active site	Gly residue allows Asp268 and Tyr394 stabilization of side chains of different substrates
N348A	Active site	Stabilization of loop that includes Met347 at the catalytic site
T349A	Active site	
P391N	Active site	This Pro is critical in the broad specificity of BsrV, allowing the stabilization of side chains from different substrates

S1*g*) can be explained by the limited interactions with Asp268 owing to their shorter side chains (Supplementary Figs. S5*c* and S5*d*). Nonetheless, additional elements seem to participate in the stabilization of basic substrates.

3.8. Functional verification of the putative specificity determinants of BsrV

To further understand the different specifities of BsrV and AlrV and to assess the significance of each 'signature' residue, we examined the activity of purified BsrV containing individual point mutations at these loci (Figs. 5*g* and 5*h* and Supplementary Figs. S5*f* and S5*g*). Notably, the mutation of any of the signature sites reduced the activity of BsrV, although the extent of the reduction varied among the mutations and among the classes of substrates (*i.e.* short and long non-β-branching aliphatic chains *versus* positively charged side chains; Fig. 5*g* and Supplementary S5*g*). Structural analysis provides likely explanations for the effects of these mutations on BsrV activity (Fig. 5*h* and Table 3). The analysis of the activity of each BsrV mutant isoform revealed that five substitutions (R119A, R121A, A165K, N167A and Y208A) reduced the activity below 20% compared with wild-type BsrV for most of the substrates (Fig. 5*g*). The footprint residues Arg119 and Arg121 are involved in salt-bridge interactions on the back side of the dimer and allow the formation of the N-terminal extension of BsrV. The dramatic effect of their absence confirms our previous conclusion (based on the P25E mutant) that the N-terminal extension is critical for the activity of BsrV towards a variety of substrates. In contrast, the A165K and N167A substitutions are expected to impair Cl^- coordination and consequently the stabilization of the catalytic Arg173. Finally, the Y208A mutant should affect the conformation of the entry loop L1 (Table 3) and, as expected, has an especially large effect on the racemization of amino acids with long side chains.

The remaining substitutions have narrower effects, and most frequently limit the activity of BsrV towards long non-β-branching amino acids, possibly because these substrates encounter more steric obstacles in entering and/or being positioned within the active site. Interestingly, a subset of mutations (G169A, N174A and P391N) that prevent the racemization of non-β-branching aliphatic amino acids do not markedly impair the activity of BsrV towards basic substrates. Based on the docking models, it seems likely that the side chains of basic substrates are stabilized by different components within the catalytic site (*e.g.* PLP, Asp268 and Tyr394; Fig. 5*e*). Analysis of a D268N mutant further confirmed that Asp268 contributes to the racemization of basic amino acids by BsrV (Supplementary Fig. S5*e*).

4. Discussion

Broad-spectrum amino-acid racemases such as BsrV enable bacteria to generate NCDAA, the varied roles of which in microbial physiology are just beginning to be appreciated (Cava, de Pedro *et al.*, 2011; Kolodkin-Gal *et al.*, 2010, 2012; Lam *et al.*, 2009). Here, we present extensive crystallographic, biochemical and bioinformatic analyses of two broad-spectrum racemases (BsrV and Bsr_{Ah}) and identify the structural features that enable such enzymes to accommodate a wider range of substrates than related PLP-dependent alanine racemases. We also identify the molecular signature for BsrV-like racemases from diverse microbes that enables them to be distinguished from monospecific alanine racemases.

Although BsrV from *V. cholerae* has previously been reported to produce primarily D-Met and D-Leu (Lam *et al.*, 2009), we found that this enzyme can also racemize eight additional amino acids typically found in proteins, as well as several nonproteinogenic amino acids. The substrates of BrsV fall into two main classes: non-β-branched aliphatic amino acids (*i.e.* Ala, Ser, Leu, Cys, Gln, Asn and Met) and basic amino acids (*i.e.* Arg, Lys and His). Although D forms of the latter class were not detected *in vivo*, kinetic analyses indicate that they can be readily generated by BsrV, perhaps facilitated by additional stabilizing interactions between these substrates and the active site of BsrV (Figs. 5*a*, 5*c* and 5*e*). Lys and Arg have also been found to be the preferred substrates of a broad-spectrum periplasmic racemase from *Pseudomonas taetrolens* (Matsui *et al.*, 2009). The enhanced active-site stabilization predicted for basic substrates may account for the resilience of the catalytic activity of mutant BsrV with such substrates relative to large uncharged aliphatic substrates

(Fig. 5*g*). The substrate range of BsrV, which includes activity towards non-natural substrates (*e.g.* ornithine, norleucine, homoserine, *N*-acetyl lysine methyl ester, diaminobutyrate and aminobutyrate; Supplementary Fig. S1*e*), is broader than any other known amino-acid racemase and suggests that it has great potential for biotechnological and industrial applications. Currently, production of DAA is an expensive process that is typically reliant upon inefficient chemical catalysts (Gong *et al.*, 2010; Green *et al.*, 2009; Toth & Richard, 2007).

Interestingly, all of the Bsr-family racemases are encoded by Gram-negative bacteria. Since some Gram-positive organisms (*e.g. B. subtilis*) have also been reported to produce NCDAA, this result suggests that additional families of broad-spectrum enzymes may remain to be identified. Consistent with this idea, the spectrum of NCDAA produced by *B. subtilis* includes several amino acids that cannot be generated by BsrV (*e.g.* D-Tyr and D-Trp; Kolodkin-Gal *et al.*, 2010). Additional broad-spectrum enzymes may not be related to the PLP-dependent racemases such as Alrs and Bsrs, but might instead bear a resemblance to other known racemases, such as MurI.

Comparative structural analyses of BsrV-family broad-spectrum racemases (BsrV and Bsr_{Ah}) and more restricted enzymes ($Alr_{Ah,}$ Alr_{Ec} and Alr_{Bs}) suggest that the catalytic plasticity of these racemases has three essential determinants: the arrangement and features of the entry site, the width of the channel leading to the active site and its catalytic environment, which is able to accommodate and stabilize substrates of diverse chemical natures. There is no indication that the underlying mechanism of racemization differs between the two enzyme subfamilies since the dominant catalytic moeties (catalytic Lys and Tyr) are found in both. The wider entry site and channel of BsrV are likely to facilitate interaction with amino-acid substrates larger than alanine; indeed, structural, biochemical and modelling analyses suggest that the entry channel of BrsV can also accommodate peptide chains which are markedly larger. The catalytic site of BsrV-like racemases is also less constrained than those of related alanine racemases, apparently owing both to differences in the components of the chambers (*e.g.* Cl^- and Pro391) and to different arrangements of the enzymatic domains that interact to form them. Previous analyses have revealed variability in the relative positioning of racemase N- and C-terminal domains owing to changes in the amino acids at the dimer interface (Couñago *et al.*, 2009). In broad-spectrum racemases, this interface is markedly altered by the presence of a new structure formed from an extended N-terminal sequence. Mutational analyses indicate that the N-terminal extension, as well as the 16 'signature' amino acids that can be used to identify broad-spectrum enzymes, are critical for racemase activity on the full set of substrates. Interestingly, mutations in most signature loci did not revert BsrV to an alanine-specific racemase; instead, its activity towards large aliphatic side chains was often lost, while its activity towards basic amino acids was preserved.

Collectively, given the impact of NCDAA on a variety of cellular processes [*e.g.* biofilm stability, sporulation and cell communication (Anfora *et al.*, 2007; Kolodkin-Gal *et al.*, 2010; O'Connor & Zusman, 1997)], structural and regulatory characterization of broad-spectrum racemases might open the door to the design of new drugs (Conti *et al.*, 2011) that would challenge the adaptability of pathogenic bacteria to adverse conditions (*i.e.* during infection).

We thank Stavroula Hatzios for insightful comments on the manuscript and Lourdes Infantes for help in data-mining analysis. Special thanks to F. Lopez-Gallego for providing DAAO. Research in the Cava laboratory is supported by the MINECO, Spain (RYC-2010-06241), Universidad Autonoma de Madrid (UAM-38) and by the Knut and Alice Wallenberg Foundation (KAW). Additionally, this work was supported by the BFU2011-25326 MEC grant (JAH), by the S2010/BMD-2457 grant from CAM (JAH) and by HHMI (MKW).

References

Adams, P. D. *et al.* (2010). *Acta Cryst.* D**66**, 213–221.
Altschul, S. F., Madden, T. L., Schäffer, A. A., Zhang, J., Zhang, Z., Miller, W. & Lipman, D. J. (1997). *Nucleic Acids Res.* **25**, 3389–3402.
Anfora, A. T., Haugen, B. J., Roesch, P., Redford, P. & Welch, R. A. (2007). *Infect. Immun.* **75**, 5298–5304.
Austin, B. (2010). *Vet. Microbiol.* **140**, 310–317.
Babtie, A., Tokuriki, N. & Hollfelder, F. (2010). *Curr. Opin. Chem. Biol.* **14**, 200–207.
Bricogne, G., Blanc, E., Brandl, M., Flensburg, C., Keller, P., Paciorek, W., Roversi, P., Smart, O. S., Vonrhein, C. & Womack, T. O. (2011). *BUSTER*. Cambridge: Global Phasing Ltd.
Cava, F., de Pedro, M. A., Lam, H., Davis, B. M. & Waldor, M. K. (2011). *EMBO J.* **30**, 3442–3453.
Cava, F., Lam, H., de Pedro, M. A. & Waldor, M. K. (2011). *Cell. Mol. Life Sci.* **68**, 817–831.
Chang, C. Y., Thompson, H., Rodman, N., Bylander, J. & Thomas, J. (1997). *Ann. Clin. Lab. Sci.* **27**, 254–259.
Chen, C. (1996). *Oral Microbiol. Immunol.* **11**, 425–427.
Chen, V. B., Arendall, W. B., Headd, J. J., Keedy, D. A., Immormino, R. M., Kapral, G. J., Murray, L. W., Richardson, J. S. & Richardson, D. C. (2010). *Acta Cryst.* D**66**, 12–21.
Chen, Y., Zhang, W., Shi, Q., Hesek, D., Lee, M., Mobashery, S. & Shoichet, B. K. (2009). *J. Am. Chem. Soc.* **131**, 14345–14354.
Conti, P., Tamborini, L., Pinto, A., Blondel, A., Minoprio, P., Mozzarelli, A. & De Micheli, C. (2011). *Chem. Rev.* **111**, 6919–6946.
Couñago, R. M., Davlieva, M., Strych, U., Hill, R. E. & Krause, K. L. (2009). *BMC Struct. Biol.* **9**, 53.
Levie, R. de (2001). *How to Use Excel in Analytical Chemistry and in General Scientific Data Analysis*. Cambridge University Press.
Delong, E. F., Franks, D. G. & Yayanos, A. A. (1997). *Appl. Environ. Microbiol.* **63**, 2105–2108.
Edgar, R. C. (2004). *Nucleic Acids Res.* **32**, 1792–1797.
El-Hajj, Z. W., Allcock, D., Tryfona, T., Lauro, F. M., Sawyer, L., Bartlett, D. H. & Ferguson, G. P. (2010). *Ann. N. Y. Acad. Sci.* **1189**, 143–148.
Emsley, P. & Cowtan, K. (2004). *Acta Cryst.* D**60**, 2126–2132.
Evans, P. (2006). *Acta Cryst.* D**62**, 72–82.
Faraci, W. S. & Walsh, C. T. (1988). *Biochemistry*, **27**, 3267–3276.
Gong, L., Mulcahy, S. P., Devarajan, D., Harms, K., Frenking, G. & Meggers, E. (2010). *Inorg. Chem.* **49**, 7692–7699.
Green, B. A., Yu, R. J. & Van Scott, E. J. (2009). *Clin. Dermatol.* **27**, 495–501.
Hanahan, D. (1985). *DNA Cloning: A Practical Approach*, Vol. 1, edited by D. M. Glover, pp. 109–135. Oxford: IRL Press.
Harris, J. B., LaRocque, R. C., Qadri, F., Ryan, E. T. & Calderwood, S. B. (2012). *Lancet*, **379**, 2466–2476.
Heidelberg, J. F. *et al.* (2000). *Nature (London)*, **406**, 477–483.
Herbert, E. E. & Goodrich-Blair, H. (2007). *Nature Rev. Microbiol.* **5**, 634–646.

Holm, L. & Rosenström, P. (2010). *Nucleic Acids Res.* **38**, W545–W549.
Horcajo, P., de Pedro, M. A. & Cava, F. (2012). *Microb. Drug Resist.* **18**, 306–313.
Howard, A., O'Donoghue, M., Feeney, A. & Sleator, R. D. (2012). *Virulence*, **3**, 243–250.
Inoue, H., Nojima, H. & Okayama, H. (1990). *Gene*, **96**, 23–28.
Jacobsen, S. M. & Shirtliff, M. E. (2011). *Virulence*, **2**, 460–465.
Kaasch, A. J., Dinter, J., Goeser, T., Plum, G. & Seifert, H. (2012). *Infection*, **40**, 185–190.
Kabsch, W. (1993). *J. Appl. Cryst.* **26**, 795–800.
Kabsch, W. (2010). *Acta Cryst.* D**66**, 125–132.
Khersonsky, O., Roodveldt, C. & Tawfik, D. S. (2006). *Curr. Opin. Chem. Biol.* **10**, 498–508.
Kim, S. E., Park, S. H., Park, H.-B., Park, K.-H., Kim, S.-H., Jung, S.-I., Shin, J.-H., Jang, H.-C. & Kang, S. J. (2012). *Chonnam Med. J.* **48**, 91–95.
Kino, K., Sato, M., Yoneyama, M. & Kirimura, K. (2007). *Appl. Microbiol. Biotechnol.* **73**, 1299–1305.
Kolodkin-Gal, I., Cao, S., Chai, L., Böttcher, T., Kolter, R., Clardy, J. & Losick, R. (2012). *Cell*, **149**, 684–692.
Kolodkin-Gal, I., Romero, D., Cao, S., Clardy, J., Kolter, R. & Losick, R. (2010). *Science*, **328**, 627–629.
Komarova, N. V., Golubev, I. V., Khoronenkova, S. V., Chubar', T. A. & Tishkov, V. I. (2012). *Biochemistry*, **77**, 1181–1189.
Laemmli, U. K. & Favre, M. (1973). *J. Mol. Biol.* **80**, 575–599.
Lam, H., Oh, D.-C., Cava, F., Takacs, C. N., Clardy, J., de Pedro, M. A. & Waldor, M. K. (2009). *Science*, **325**, 1552–1555.
LeMagueres, P., Im, H., Dvorak, A., Strych, U., Benedik, M. & Krause, K. L. (2003). *Biochemistry*, **42**, 14752–14761.
LeMagueres, P., Im, H., Ebalunode, J., Strych, U., Benedik, M. J., Briggs, J. M., Kohn, H. & Krause, K. L. (2005). *Biochemistry*, **44**, 1471–1481.
Lenk, S., Moraru, C., Hahnke, S., Arnds, J., Richter, M., Kube, M., Reinhardt, R., Brinkhoff, T., Harder, J., Amann, R. & Mussmann, M. (2012). *ISME J.* **6**, 2178–2187.
Long, F., Vagin, A. A., Young, P. & Murshudov, G. N. (2008). *Acta Cryst.* D**64**, 125–132.
Matsui, D. & Oikawa, T. (2010). *Chem. Biodivers.* **7**, 1591–1602.
Matsui, D., Oikawa, T., Arakawa, N., Osumi, S., Lausberg, F., Stäbler, N., Freudl, R. & Eggeling, L. (2009). *Appl. Microbiol. Biotechnol.* **83**, 1045–1054.
Murakami, K. (2012). *J. Gastroenterol.* **47**, 724–725.
Nelson, M. D. & Fitch, D. H. (2011). *Methods Mol. Biol.* **772**, 459–470.
Noda, M., Matoba, Y., Kumagai, T. & Sugiyama, M. (2004). *J. Biol. Chem.* **279**, 46153–46161.
O'Connor, K. A. & Zusman, D. R. (1997). *Mol. Microbiol.* **24**, 839–850.
O'Hara, C. M., Brenner, F. W. & Miller, J. M. (2000). *Clin. Microbiol. Rev.* **13**, 534–546.
Pepperell, C., Kus, J. V., Gardam, M. A., Humar, A. & Burrows, L. L. (2002). *Antimicrob. Agents Chemother.* **46**, 3555–3560.
Pinhassi, J., Pujalte, M. J., Macián, M. C., Lekunberri, I., González, J. M., Pedrós-Alió, C. & Arahal, D. R. (2007). *Int. J. Syst. Evol. Microbiol.* **57**, 2370–2375.
Richard, J. P., Amyes, T. L., Crugeiras, J. & Rios, A. (2009). *Curr. Opin. Chem. Biol.* **13**, 475–483.
Rømer Villumsen, K., Dalsgaard, I., Holten-Andersen, L. & Raida, M. K. (2012). *PLoS One*, **7**, e46733.
Rosenberg, A. H., Lade, B. N., Chui, D.-S., Lin, S.-W., Dunn, J. J. & Studier, F. W. (1987). *Gene*, **56**, 125–135.
Rózalski, A., Kwil, I., Torzewska, A., Baranowska, M. & Staczek, P. (2007). *Postepy Hig. Med. Dosw. (Online)*, **61**, 204–219.
Seifert, H., Strate, A., Schulze, A. & Pulverer, G. (1993). *Clin. Infect. Dis.* **17**, 632–636.
Shaw, J. P., Petsko, G. A. & Ringe, D. (1997). *Biochemistry*, **36**, 1329–1342.
Strych, U. & Benedik, M. J. (2002). *J. Bacteriol.* **184**, 4321–4325.
Su, Y.-C. & Liu, C. (2007). *Food Microbiol.* **24**, 549–558.
Sugar, D. R., Murfin, K. E., Chaston, J. M., Andersen, A. W., Richards, G. R., deLéon, L., Baum, J. A., Clinton, W. P., Forst, S., Goldman, B. S., Krasomil-Osterfeld, K. C., Slater, S., Stock, S. P. & Goodrich-Blair, H. (2012). *Environ. Microbiol.* **14**, 924–939.
Timoney, P. J. (1996). *Comp. Immunol. Microbiol. Infect. Dis.* **19**, 199–204.
Toth, K. & Richard, J. P. (2007). *J. Am. Chem. Soc.* **129**, 3013–3021.
Vagin, A. & Teplyakov, A. (2010). *Acta Cryst.* D**66**, 22–25.
Vollmer, W., Blanot, D. & de Pedro, M. A. (2008). *FEMS Microbiol. Rev.* **32**, 149–167.
Watanabe, A., Yoshimura, T., Mikami, B., Hayashi, H., Kagamiyama, H. & Esaki, N. (2002). *J. Biol. Chem.* **277**, 19166–19172.
Williamson, E. D. & Oyston, P. C. (2012). *J. Med. Microbiol.* **61**, 911–918.
Waterhouse, A. M., Procter, J. B., Martin, D. M. A., Clamp, M. & Barton, G. J. (2009). *Bioinformatics*, **25**, 1189–1191.
Winn, M. D. *et al.* (2011). *Acta Cryst.* D**67**, 235–242.
Wu, D., Hu, T., Zhang, L., Chen, J., Du, J., Ding, J., Jiang, H. & Shen, X. (2008). *Protein Sci.* **17**, 1066–1076.
Zhao, J.-S., Manno, D., Leggiadro, C., O'Neil, D. & Hawari, J. (2006). *Int. J. Syst. Evol. Microbiol.* **56**, 205–212.